Journal of Applied Physics

Evaluation of the precursor decay anomaly in single crystal lithium fluoride

Cite as: J. Appl. Phys. **106**, 023534 (2009); https://doi.org/10.1063/1.3159655
Submitted: 23 May 2009 • Accepted: 03 June 2009 • Published Online: 29 July 2009

Yukio Sano and Tomokazu Sano

AIP Publishing

Evaluation of the precursor decay anomaly in single crystal lithium fluoride

Yukio Sano[1,a)] and Tomokazu Sano[2]
[1]*38-10, Shibatani-Cho, Takatsuki, Osaka 569-1025, Japan*
[2]*Department of Manufacturing Science, Graduate School of Engineering, Osaka University, Suita, Osaka 565-0871, Japan*

(Received 23 May 2009; accepted 3 June 2009; published online 29 July 2009)

To decide whether many dislocations are generated in lithium fluoride (LiF III_b) and to examine whether the precursor decay anomaly exists, an equation that predicts the dislocation densities on the precursor decay curve without using any modeled dislocation generation rate has been derived. The value of the density of at most about 2.0×10^{12} m^{-2} evaluated on the decay curve in the material III_b for a projectile velocity of 340 m/s indicates that extremely many dislocations are not generated in the material. This value is not significantly larger than the value of about 10^{10} m^{-2} measured at a projectile velocity of 186 m/s. It is inferred from the evaluated value of 2.0×10^{12} m^{-2} that the measured value of 10^{10} m^{-2} is not unreasonable and therefore that the precursor decay anomaly does not exist. In addition, it has been revealed that dislocation densities largely increase on the decay curve. © *2009 American Institute of Physics*. [DOI: 10.1063/1.3159655]

I. INTRODUCTION

The precursor decay anomaly in single crystal lithium fluoride (LiF) posed by Duvall and coworkers[1–3] in 1972 is one of the most scientific questions in shock wave physics. The anomaly means extremely large difference in value between the measured dislocation density and the density at the impacted surface on the precursor decay curve calculated assuming impact between elastic bodies. An effort was made to resolve the anomaly. By simulating their experiments taking into consideration the generations of dislocations at the impact and rear surfaces of the pure crystal LiF sample and at the subgrain boundaries in the sample, Meir and Clifton[4] suggested that the generations reduced the anomaly. Partom[5] performed calculations of decay flow fields and precursor decay curves for 2024-T351Al and suggested that if a finite rate of dislocation generation was assumed, the anomaly was reduced.

Sano[6–8] made an effort to resolve the anomaly in a single crystal LiF material (III_b) (Ref. 1) using an approach that differed from those of Meir and Clifton[4] and Partom.[5] The dislocation density on the decay curve at the impacted surface estimated by Sano[6] was extremely higher than the densities in recovered samples measured by Vorthman and Duvall.[3] He[6] considered that the anomaly was due to having based calculations on the extremely high and steep Asay's decay curve that started upon shock loading.[1] In his quantitative analysis of a smooth plane wave front in the vicinity of the impact surface, Sano[7] revealed that the stress amplitude of the steady precursor in the wave front increased from the Hugoniot elastic limit to a maximum value and then decreased. The Sano's decay curve obtained under the inference that it started from the maximum amplitude point was much lower than the Asay's decay curve. Sano[8] quantitatively analyzed the decay process in the material III_b. This analysis revealed that as the decay was slow, the plastic strain rate at the leading edge of the follower was small. Thus, the studies of Sano[6–8] demonstrated that the anomaly was reduced by using the Sano's decay curve in the analysis.

In spite of the effort of the resolve of the anomaly by Sano,[6–8] extremely high dislocation densities were recently reported by Gilman,[9] Shehadeh *et al.*[10] (about 10^{15} m^{-2} in 1 ns), and Bringa *et al.*[11] (about 10^{18} m^{-2}). However, a question arises as to whether or not so many dislocations are generated in LiF. To answer this question, it is at least required to formulate an equation by which dislocation densities can be predicted without relying on any modeled dislocation generation rate. It is possible to derive an equation for the density on the precursor decay curve. This equation should predict dislocations that are more on the Asay's decay curve than on the Sano's curve. If dislocation densities on the Asay's decay curve evaluated from the equation are not sufficiently high, many dislocations are decided not to be generated in LiF, meaning that the anomaly does not exist.

In this study, we derive an equation that predicts the dislocation densities at the leading edge of the follower on the decay curve without using any modeled dislocation generation rate. In addition, we derive an inequality for the density at the rear of the precursor on the curve. Next, by estimating the changes in time of the densities at the rear and at the leading edge on the Sano's decay curve, it is revealed that the density largely increases near the leading edge. Finally, the densities at the leading edge on the Asay's decay curve are calculated. Based on the maximum value at the impacted surface evaluated, it is decided whether extremely many dislocations are generated in LiF III_b and inferred whether the anomaly exists.

II. THEORETICAL BACKGROUND

In this section, the equations for the particle velocity and the stress waves derived by Sano[8] are described, together with the equations for the relaxation function and the dislo-

[a)]Electronic mail: profeme_ys@yahoo.co.jp.

cation density derived by Sano.[6] They are used in formulating the dislocation density on the decay curve in Sec. III.

A. Strain, particle velocity, and stress waves

Sano[8] derived equations for the particle velocity and the stress waves, which correspond to linear stain waves, in the precursor and in the front part of the follower in a weak-discontinuity plane wave front during the decay process.[12] He[8] used a moving coordinate system expressed by

$$\xi = h - \tau, \quad \tau = \int_0^q c(q)dq,$$

where h is the initial or Lagrangian position at time $t=0$, at which the specimen is impacted, q is the time that begins from the time t_s when a kink has occurred in a smooth plane wave, that is, $q=t-t_s(\geqslant 0)$, and $c(q)$ is the velocity of the leading edge of the follower. The equation for the linear strain wave in the precursor $[0<\xi\leqslant\xi_f]$ is

$$\varepsilon(\xi,q) = \varepsilon_i - \frac{\varepsilon_i}{\xi_f}\xi, \tag{1}$$

where $\varepsilon(\xi,q)\equiv\varepsilon(\xi,\tau)\equiv\tilde{\varepsilon}(h,q)$, $\varepsilon_i(q)[\equiv\varepsilon(0,q)\equiv\tilde{\varepsilon}(h_i,q)]$ is the strain at the leading edge of the follower on a precursor decay curve, whose location is expressed by $h=h_i(q)$ or $\xi=0$, and $\xi_f(q)$ is the location of the leading edge of the precursor or the thickness of the precursor. The equation for the particle velocity wave corresponding to the strain wave is

$$v(\xi,q) = v_i - \left(\frac{c\varepsilon_i}{\xi_f} + \dot{\varepsilon}_i\right)\xi + \frac{\dot{\varepsilon}_i\xi_f - \varepsilon_i\dot{\xi}_f}{2\xi_f^2}\xi^2, \tag{2}$$

where $v(\xi,q)\equiv v(\xi,\tau)\equiv\tilde{u}(h,q)$, the dots over the variables refer to differentiation with respect to q, $v_i(q)$ is the particle velocity at the leading edge of the follower expressed by $v_i=c\varepsilon_i+(\dot{\varepsilon}_i\xi_f+\varepsilon_i\dot{\xi}_f)/2$, and $\dot{\xi}_f=c_f-c$, where $c_f(q)$ is the velocity of the leading edge of the precursor. The equation for the stress wave corresponding to the strain wave is

$$\sigma(\xi,q) = \sigma_i + \rho_0\left\{\left(-\frac{c^2\varepsilon_i}{\xi_f} + A\right)\xi + B\xi^2 + D\xi^3\right\}, \tag{3}$$

where $\sigma(\xi,q)\equiv\sigma(\xi,\tau)\equiv\tilde{\sigma}(h,q)$, $\sigma_i(q)$ is the stress at the leading edge of the follower expressed by $\sigma_i=\rho_0(c^2\varepsilon_i-A\xi_f-B\xi_f^2-D\xi_f^3)$. As for coefficients $A(q)$, $B(q)$, and $D(q)$, see Ref. 6.

The equation for the linear strain wave in the follower $[\xi\leqslant 0]$ is

$$\varepsilon(\xi,q) = \varepsilon_i - \gamma\xi, \tag{4}$$

where $\gamma(q)$ is the angle of incidence of the strain wave. The equations for the particle velocity and the stress waves corresponding to the strain wave are

$$v(\xi,q) = v_i - (c\gamma + \dot{\varepsilon}_i)\xi + \tfrac{1}{2}\dot{\gamma}\xi^2, \tag{5}$$

$$\sigma(\xi,q) = \sigma_i + \rho_0(E\xi + F\xi^2 + G\xi^3). \tag{6}$$

As for coefficients $E(q)$, $F(q)$, and $G(q)$, see Ref. 6.

B. Dislocation density

Sano[6] derived an equation for stress relaxation function $F(h,q)$ by incorporating the equations of conservation of mass and momentum into the constitutive relation of Duvall,[13]

$$\alpha\frac{D\tilde{\sigma}}{Dq} + (1-\alpha)\left(\frac{\partial\tilde{\sigma}}{\partial q}\right)_h = -2\mu\left(\frac{\partial\tilde{e}^p}{\partial q}\right)_h = -F, \tag{7}$$

where D/Dq represents differentiation along a path in time $[h=h_\sigma(q)]$ in the (h,q) coordinate system and $\tilde{e}^p(h,q)$ is the plastic component of the natural strain in the direction of wave propagation $\tilde{e}(h,q)$, μ is the shear modulus, and $\alpha(h,q)$ is the velocity ratio expressed by

$$\alpha = \frac{c_L^{\,2}}{c_\sigma c_{uc}}, \tag{8}$$

where $c_\sigma\equiv dh_\sigma/dq$ (Ref. 6) and $c_{uc}(h,q)$ is the phase velocity at a constant particle velocity derived by Fowles,[14] which is expressed by

$$c_{uc} = -\frac{(\partial\tilde{u}/\partial q)_h}{(\partial\tilde{u}/\partial h)_q}, \tag{9}$$

and where $c_L(h,q)$ is the Lagrangian wave speed in a uniaxial strain state expressed by $c_L=(\rho_0/\tilde{\rho})\tilde{a}$, where ρ_0 is the initial material density, $\tilde{\rho}(h,q)$ is the material density, and $\tilde{a}$ is the Eulerian wave speed.

Asay *et al.*[1] and Gupta *et al.*[2] related the relaxation function F to the dislocation density N_m,

$$N_m = \eta F, \tag{10}$$

where $\eta=1/(2\mu b v_d)$, where b is the Burgers vector and v_d is the average dislocation velocity expressed by $v_d=v_s\exp(-D/\tau_r)$, where v_s is the shear wave velocity, D is the drag stress, and τ_r is the resolved shear stress that is related to stress σ by $\tau_r=(221/760)\sigma$ in LiF. For LiF III_b, we have $b=2.85\times10^{-10}$ m, $\mu=11.05$ GPa, and therefore $\eta\cong 10/(63v_d)$ $\mathrm{Pa^{-1}\,s\,m^{-2}}$, and $v_s=3280$ m/s. The value of D is discussed in Sec. IV B.

C. Validity of use of the constitutive relation of Duvall

Since the assumption that stresses are maintained by elastic strains alone is used in deriving the constitutive relation of Duvall,[13] strain rate and acceleration must not be included in $\tilde{\sigma}$ in Eq. (7). Armstrong *et al.*[15] interpreted the dislocation generation rate to be of controlling importance in constitutive equation modeling of shock-induced plasticity. This means that the effects of strain rate and acceleration are included in shock-induced stress $\tilde{\sigma}$. However, the effects on the stress on the decay curve, that is, on the stress at the rear of the near elastic precursor are small. Therefore, Eq. (7) holds on the decay curve to a good approximation.

III. FORMULATION OF DISLOCATION DENSITIES ON THE DECAY CURVE

In this section, an equation for the relaxation function at the leading edge of the follower is first derived from Eq. (7) using Eqs. (5) and (6). Next, an inequality for the function at

the rear of the precursor is derived, and then expressions for the lower and upper bounds of the inequality are obtained using Eqs. (1)–(3).

A. At the leading edge of the follower

The following equation for the relaxation function $F_i[\equiv F(h_i)]$ at the leading edge of the follower on the decay curve is obtained from Eq. (7):

$$\alpha_i \dot{\sigma}_i + (1-\alpha_i)\left(\frac{\partial \tilde{\sigma}}{\partial q}\right)_{h,h=h_i} = -F_i, \tag{11}$$

where $F_i = 2\mu(\partial \tilde{e}^p/\partial q)_{h,h=h_i}$, and $\alpha_i \equiv \alpha(h_i) = {c_{Li}}^2/(c_{\sigma i}c_{uci})$ is obtained from Eq. (8), where $c_{Li} \equiv c_L(h_i)$, $c_{uci} \equiv c_{uc}(h_i)$, and $c_{\sigma i} \equiv dh_i/dq \equiv c$. In Eq. (7), D/Dq represented the differentiation along the path $[h=h_\sigma(q)]$, but in Eq. (11), it is along the decay curve, so that $D\tilde{\sigma}/Dq$ in Eq. (7) becomes $\dot{\sigma}_i(q)$ in Eq. (11). Since the velocity of the leading edge of the follower c is the Lagrangian wave speed, that is, since $c_{Li} \equiv c$, the relation for α_i, which is obtained from Eq. (8), reduces to

$$\alpha_i = \frac{c}{c_{uci}}. \tag{12}$$

An equation for α_i is first derived. Equation $c_{uci} = c[1 - (\partial v/\partial \tau)_{\xi,\xi=0}/(\partial v/\partial \xi)_{\tau,\xi=0}]$ is obtained from Eq. (9), where $(\partial v/\partial \tau)_{\xi,\xi=0} = \dot{v}_i/c$ and $(\partial v/\partial \xi)_{\tau,\xi=0} = -c\gamma - \dot{\varepsilon}_i$, which were obtained from Eq. (5). Substitution of the equation for c_{uci} above into Eq. (12) yields

$$\alpha_i = \frac{c(c\gamma + \dot{\varepsilon}_i)}{c(c\gamma + \dot{\varepsilon}_i) + \dot{v}_i}. \tag{13}$$

Next, equation $(\partial \tilde{\sigma}/\partial q)_{h,h=h_i} = -\rho_0 cE + \dot{\sigma}_i$ is derived using $(\partial \sigma/\partial \xi)_{\tau,\xi=0} = \rho_0 E$ $(E = -c^2\gamma - c\dot{\varepsilon}_i - \dot{v}_i)$ and $(\partial \sigma/\partial \tau)_{\xi,\xi=0} = \dot{\sigma}_i/c$, which are obtained from Eq. (6). Finally, substitution of Eq. (13) and the equation for $(\partial \tilde{\sigma}/\partial q)_{h,h=h_i}$ above into Eq. (11) yields an equation for F_i,

$$F_i = -(\rho_0 c\dot{v}_i + \dot{\sigma}_i). \tag{14}$$

The same equation as the equation above is also derived from the strain wave in the follower that is expressed by a power series up to the nth $(\geqslant 2)$ order with respect to ξ.

The equation for the dislocation density at the leading edge of the follower $N_{mi}[\equiv N_m(h_i)]$ is

$$N_{mi} = \eta_i F_i, \tag{15}$$

where $\eta_i = 10/(63v_{di})$. Here $v_{di} = v_s \exp(-D/\tau_{ri})$, where $\tau_{ri} = (221/760)\sigma_i$.

B. At the rear of the precursor

The equation for the function F_i^+ $[\equiv F(h_i^+)]$ at the rear of the precursor, whose location is expressed by $h = h_i(q)^+$ or $\xi = 0^+$, is[6]

$$\alpha_i^+ \dot{\sigma}_i + (1-\alpha_i^+)\left(\frac{\partial \tilde{\sigma}}{\partial q}\right)_{h,h=h_i^+} = -F_i^+, \tag{16}$$

where $F_i^+ = 2\mu(\partial \tilde{e}^p/\partial q)_{h,h=h_i^+}$, and α_i^+ $[\equiv \alpha(h_i^+)]$ satisfies inequalities

$$\alpha_{il} \leqslant \alpha_i^+ \leqslant \alpha_{iu}, \tag{17}$$

where α_{il} is the lower bound of α_i^+ and α_{iu} is the upper bound. The lower bound is given by $\alpha_{il} \equiv \alpha_{\varepsilon il}$, $\alpha_{il} \equiv \alpha_{uil}$, or $\alpha_{il} \equiv \alpha_{\sigma il}$, where $\alpha_{\varepsilon il} = {c_{\varepsilon ci}}^2/(c_{\sigma i}c_{uci})$, $\alpha_{uil} = c_{uci}/c_{\sigma i}$, and $\alpha_{\sigma il} = {c_{\sigma ci}}^2/(c_{\sigma i}c_{uci})$, where $c_{\varepsilon ci} \equiv c_{\varepsilon c}(h_i^+)$, $c_{uci} \equiv c_{uc}(h_i^+)$, and $c_{\sigma ci} \equiv c_{\sigma c}(h_i^+)$ are the phase velocities at constant strain, constant particle velocity, and constant stress at the rear of the precursor, respectively,[6] which are expressed as

$$c_{\varepsilon ci} = c\left\{1 - \frac{(\partial \varepsilon/\partial \tau)_{\xi,\xi=0^+}}{(\partial \varepsilon/\partial \xi)_{\tau,\xi=0^+}}\right\}, \quad c_{uci} = c\left\{1 - \frac{(\partial v/\partial \tau)_{\xi,\xi=0^+}}{(\partial v/\partial \xi)_{\tau,\xi=0^+}}\right\},$$

$$c_{\sigma ci} = c\left\{1 - \frac{(\partial \sigma/\partial \tau)_{\xi,\xi=0^+}}{(\partial \sigma/\partial \xi)_{\tau,\xi=0^+}}\right\}.$$

The following relations are derived from Eqs. (1)–(3), respectively,

$$(\partial \varepsilon/\partial \tau)_{\xi,\xi=0^+} = \dot{\varepsilon}_i/c, \quad (\partial \varepsilon/\partial \xi)_{\tau,\xi=0^+} = -\varepsilon_i/\xi_f,$$

$$(\partial v/\partial \tau)_{\xi,\xi=0^+} = \dot{v}_i/c, \quad (\partial v/\partial \xi)_{\tau,\xi=0^+} = -c\varepsilon_i/\xi_f - \dot{\varepsilon}_i,$$

$$(\partial \sigma/\partial \tau)_{\xi,\xi=0^+} = \dot{\sigma}_i/c, \quad (\partial \sigma/\partial \xi)_{\tau,\xi=0^+} = \rho_0(-c^2\varepsilon_i/\xi_f + A).$$

On the other hand, if the precursor is not overtaken by the follower during the decay process, that is, if the rear of the precursor attenuates in the same manner as the leading edge of the follower, α_i^+ becomes a maximum, that is, $\alpha_i^+ = \alpha_{iu}$, where $\alpha_{iu} \equiv \alpha(h_i^+) = {c_L(h_i^+)}^2/\{c_{\sigma i}c_{uc}(h_i^+)\}$, where $c_{\sigma i} \equiv dh_i/dq \equiv c$.

As shown by Asay *et al.*,[1] Gupta *et al.*,[2] and Sano,[7] the precursor is not perfectly steady, so that $\alpha_{\varepsilon il} \neq \alpha_{uil} \neq \alpha_{\sigma il}$. Calculations, which are performed in Sec. IV C, indicate $\alpha_{\varepsilon il} > \alpha_{uil} > \alpha_{\sigma il}$. Therefore, it is found from inequality (17) that $\alpha_{il} \equiv \alpha_{\varepsilon il}$, and as a result, we have

$$\alpha_{il} = \frac{{c_{\varepsilon ci}}^2}{cc_{uci}}. \tag{18}$$

Since $c_L(h_i^+) \equiv c_{\sigma i} \equiv c$, the upper bound α_{iu} reduces to

$$\alpha_{iu} = \frac{c}{c_{uc}(h_i^+)}. \tag{19}$$

Since inequality $(\partial \tilde{\sigma}/\partial q)_{h,h=h_i^+} - \dot{\sigma}_i > 0$ holds for the precursor, which is the wave C, application of inequality (17) to α_i^+ in Eq. (16) yields

$$F_{il} \leqslant F_i^+ \leqslant F_{iu}, \tag{20}$$

where the equation for the lower bound F_{il} is

$$F_{il} = \alpha_{il}\left\{\left(\frac{\partial \tilde{\sigma}}{\partial q}\right)_{h,h=h_i^+} - \dot{\sigma}_i\right\} - \left(\frac{\partial \tilde{\sigma}}{\partial q}\right)_{h,h=h_i^+}. \tag{21}$$

Substitution of Eq. (18) and the equation for $(\partial \tilde{\sigma}/\partial q)_{h,h=h_i^+}$, which is obtained from Eq. (3), into Eq. (21) yields

$$F_{il} = \rho_0\left\{\left(c + \frac{\dot{\varepsilon}_i\xi_f}{\varepsilon_i}\right)\left(2c + \frac{\dot{\varepsilon}_i\xi_f}{\varepsilon_i}\right)\dot{\varepsilon}_i - c\dot{v}_i\right\} - \dot{\sigma}_i. \tag{22}$$

On the other hand, the equation for the upper bound F_{iu} is

$$F_{iu} = \alpha_{iu}\left\{\left(\frac{\partial\tilde{\sigma}}{\partial q}\right)_{h,h=h_i^+} - \dot{\sigma}_i\right\} - \left(\frac{\partial\tilde{\sigma}}{\partial q}\right)_{h,h=h_i^+}. \quad (23)$$

By substituting Eq. (19) and the equation for $(\partial\tilde{\sigma}/\partial q)_{h,h=h_i^+}$, which is obtained from Eq. (3), into Eq. (23), an equation is obtained,

$$F_{iu} = -(\rho_0 c\dot{v}_i + \dot{\sigma}_i). \quad (24)$$

The same equation as the equation above is also derived from the strain wave in the precursor that is expressed by a power series up to the nth ($\geqslant 2$) order with respect to ξ. Equation (24) is identical to Eq. (14), namely,

$$F_{iu} \equiv F_i. \quad (25)$$

The identity of F_{iu} to F_i is justified by the fact that the form and the slope of the precursor are not included in the equation for F_{iu}, as well as the fact that those of the follower are not in the equation for F_i. If $\dot{\sigma}_i \cong \rho_0 c\dot{v}_i$, then $F_{iu} \cong -2\dot{\sigma}_i$, so that $0 < F_i^+ \leqslant -2\dot{\sigma}_i$ for a thin precursor.

The following inequalities are obtained for the dislocation density at the rear of the precursor $N_{mi}^+[\equiv N_m(h_i^+)]$:

$$N_{mil} \leqslant N_{mi}^+ \leqslant N_{miu}, \quad (26)$$

where $N_{mil} = \eta_i F_{il}$ and $N_{miu} = \eta_i F_{iu}$. From Eq. (25),

$$N_{miu} \equiv N_{mi}. \quad (27)$$

C. Results extracted from Eq. (14)

Three important results are extracted from Eq. (14). This equation only includes the slopes of the decay curves for particle velocity and stress as variables. Thus, the relaxation function is independent of the form and the angle of incidence of the follower. Therefore, the first result extracted is that Eq. (14) holds irrespective of the kind of the follower [contraction (compression) wave C, degenerate contraction waves I and II, subrarefaction wave R', and rarefaction wave R_b]. This is justified by the demonstration of Sano[6] that the constitutive relation of Duvall[13] holds in any of the five elementary waves. The jumps in particle velocity and stress across the precursor in LiF III$_b$ both satisfy the Rankine–Hugoniot (RH) jump conditions, $\dot{v}_i = c\dot{\varepsilon}_i$ and $\dot{\sigma}_i = \rho_0 c^2 \dot{\varepsilon}_i$, to a good approximation,[8] indicating that if the ε_i-t curve is steep, then both the v_i-t and σ_i-t curves are also steep and hence the value of F_i is large at any time during the decay process. In short, Eq. (14) implies that as the decay is steep, plastic strain rate is large. Therefore, it is found easily from Eq. (14) that the values of F_i are larger along the Asay's decay curve than along the Sano's decay curve. This is the second extracted, although it was already revealed in the analysis of Sano.[8] If the decay curve is accurately determined, relaxation functions would be precisely evaluated from Eq. (14) because neither the form nor the angle of incidence of the follower are included in the equation for the function as mentioned above in this paragraph. This is the third (final) extracted.

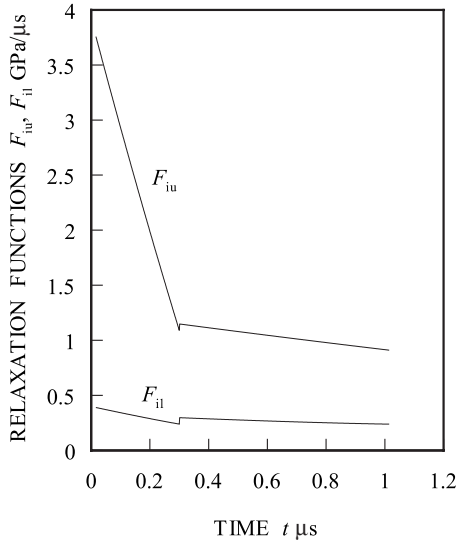

FIG. 1. Changes in time of F_{il} and F_{iu}. Symbols F_{il} and F_{iu} represent the lower and upper bounds of the relaxation function at the rear of the precursor on the Sano's decay curve, respectively. The upper bound F_{iu} is identical to the function at the leading edge of the follower F_i.

IV. DISLOCATION DENSITIES ALONG THE SANO'S DECAY CURVE

In this section, F_i is calculated from Eq. (14) or Eq. (24), and F_{il} from Eq. (22). In these equations, c, ξ_f, and ε_i are included. As for c and ξ_f, the expressions determined by Sano[8] are used. For ε_i, see Appendix.

A. Relaxation function

Changes in time of the lower and upper bounds of the relaxation function F_{il} and F_{iu} ($\equiv F_i$) at the rear of the precursor on the Sano's decay curve are shown in Fig. 1. The follower is the wave C from t=0.015 to 0.055 μs, the wave I from 0.055 to 0.057 μs, the wave II from 0.057 to 0.063 μs, the wave R' from 0.063 to 0.095 μs, and the wave R_b after 0.095 μs.[8] At any point on the decay curve, the value of the function F_i is considerably larger than that of the lower bound F_{il}, irrespective of the kind of the follower. As is inferred from the fact that the linear current-time profiles for the precursors measured by Asay *et al.*[1] have almost the same slope, the precursor is a near-steady wave, which does not attenuate greatly,[1,2,7] indicating that at any time in the decay process, the value of the function at the rear of the precursor F_i^+ is not remarkably larger than that of the lower bound, that is, $F_i^+ \cong F_{il}$. Therefore, the difference in value between the functions F_i and F_i^+ is large. The large difference means that the decay is caused mainly by the follower overtaking the precursor and that plastic flow increases greatly near the leading edges of the followers C, I, II, R', and R_b.

B. Drag effects

Under shock conditions in which the resolved shear stresses are much larger than the static yield stress, dislocation velocities v_d may be so rapid that they are comparable with the shear wave velocity v_s. In order that rapid disloca-

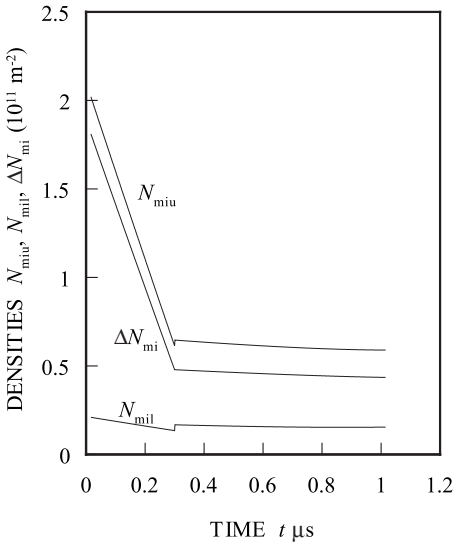

FIG. 2. Changes in time of N_{mil}, N_{miu}, and $\Delta N_{mi}(=N_{miu}-N_{mil})$, where N_{mil} and N_{miu} are the lower and upper bounds of the dislocation density at the rear of the precursor on the Sano's decay curve, respectively. The upper bound N_{miu} is identical to the density at the leading edge of the follower N_{mi}.

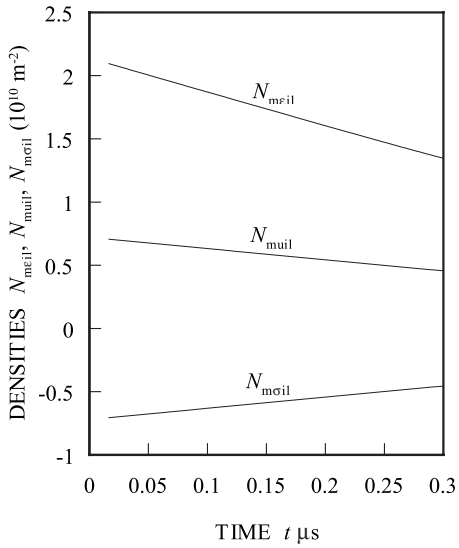

FIG. 3. Changes in time of three different lower bounds at the rear of the precursor on the Sano's decay curve, $N_{m\varepsilon il}$, N_{muil}, and $N_{m\sigma il}$.

tion velocities are predicted from $v_d=v_s\exp(-D/\tau_r)$,[2,16,17] small values of the drag stress D are required. In fact, there is a small critical value of $D_{cr}=0.036$ GPa. The change in time of the density N_{mi} for any value of D in a range of $D\geqslant D_{cr}$ increases with time after a time between $t=0.3$ and $t=1.0$ μs, which approaches to 1.0 μs as the value of D decreases to the value of D_{cr}. The reason for the occurrence of such unreasonable changes is that the value of the function F_i becomes small with time (see Fig. 1), whereas the value of the coefficient η_i becomes large. In other words, for any value of D in a range of $D\leqslant D_{cr}$, we predict a reasonable N_{mi} distribution that decreases with time up to $t=1.0$ μs, indicating that values of D in the range of $D\leqslant D_{cr}$ should be used. In the next section, calculations are performed using the value of $D=0.036$ GPa.

Velocity $v_{di}\cong 2670$ m/s is calculated from $v_{di}=v_s\exp(-D/\tau_{ri})$ using the values of $D=0.036$ GPa and $\tau_{ri}=(221/760)\sigma_i$ obtained from a middle value $\sigma_i=0.6$ GPa between the values of stresses σ_i at $t=0.3$ and $t=1.0$ μs. The velocity of 2670 m/s comparable with $v_s=3280$ m/s obtained illustrates the indication of Granato[16] that dislocation drag effects are not effective under shock loading conditions.

C. Dislocation density

Changes in time of the lower and upper bounds of the dislocation density N_{mil} and N_{miu} $(\equiv N_{mi})$ at the rear of the precursor on the Sano's decay curve are shown in Fig. 2. The density N_{mi} decreases rapidly with time from a maximum value of about 2.0×10^{11} m^{-2} at $t=0.015$ μs to a value of about 0.65×10^{11} m^{-2} at $t=0.3$ μs. This rapid decrease in N_{mi} is evident from changes in time of $\dot{v}_i$ and $\dot{\sigma}_i$ included in Eq. (24), whose absolute values decrease rapidly up to 0.3 μs.

Figure 2 also shows a change in time of the difference $\Delta N_{mi}=N_{miu}-N_{mil}$. Since $F_i^+\cong F_{il}$ (see Sec. IV A), we have $N_{mi}^+\cong N_{mil}$ and hence $\Delta N_{mi}\cong N_{mi}-N_{mi}^+$. The large values of ΔN_{mi}, which are shown in Fig. 2, reveal that the density increases largely near the leading edge of the follower. This large increase results from the generations of dislocations near the impact surface and at the subgrain boundaries as well as in the bulk.[4,5]

Figure 3 shows changes in time of three different lower bounds, $N_{m\varepsilon il}$, N_{muil}, and $N_{m\sigma il}$, calculated up to $t=0.3$ μs, where $N_{m\varepsilon il}=\eta_i F_{\varepsilon il}$, $N_{muil}=\eta_i F_{uil}$, and $N_{m\sigma il}=\eta_i F_{\sigma il}$, where $F_{\varepsilon il}$, F_{uil}, and $F_{\sigma il}$ are given by Eq. (21) where $\alpha_{il}\equiv\alpha_{\varepsilon il}$, $\alpha_{il}\equiv\alpha_{uil}$, and $\alpha_{il}\equiv\alpha_{\sigma il}$, respectively. The negative values of $N_{m\sigma il}$ have no physical meaning. As shown in Fig. 3, inequalities $N_{m\varepsilon il}>N_{muil}>N_{m\sigma il}$ hold, indicating that $N_{mil}\equiv N_{m\varepsilon il}$. The density N_{mil} decreases almost linearly with time from a maximum value of about 2.1×10^{10} m^{-2} at the beginning to a value of about 1.3×10^{10} m^{-2} at $t=0.3$ μs. The values of N_{mi}^+ $[\cong(2.1-1.3)\times10^{10}$ m$^{-2}]$ are considerably larger than that of the initial density $(2-10)\times10^8$ m^{-2} in the bulk. The dislocation generations near the impact surface and at the subgrain boundaries as well as in the bulk are also responsible for the larger values of N_{mi}^+.

V. PRECURSOR DECAY ANOMALY

A. Dislocation generation

The densities N_{mi} on the Asay's decay curve that begins at $t=0$ are evaluated from Eq. (15). The strain ε_s induced at the impacted surface upon shock loading has a value of $\varepsilon_s\cong0.024$ that is obtained from the RH jump condition $\tilde{u}_{max}=c_0\varepsilon_s$ using $c_0\cong7000$ m/s and $\tilde{u}_{max}\cong166$ m/s, where c_0 is the velocity of an shock-induced wave at $t=0$ and $\tilde{u}_{max}$ is the peak particle velocity at the impacted surface.[18] A change in time of N_{mi} for $\varepsilon_s=0.024$ is shown by a dashed line in Fig. 4. However, Sano[7] revealed $\tilde{u}_{max}=0.80c_0\varepsilon_s$ at the impacted surface. In this case, the value of ε_s is $\varepsilon_s\cong0.030$. A change in time of N_{mi} for $\varepsilon_s=0.030$ is shown by a solid line. The difference in value between both the changes is not large. The value of the density N_{mi} decreases from about 2.0×10^{12} at $t=0$ to about 0.3×10^{11} m^{-2} at $t=0.3$ μs. The value of 2.0

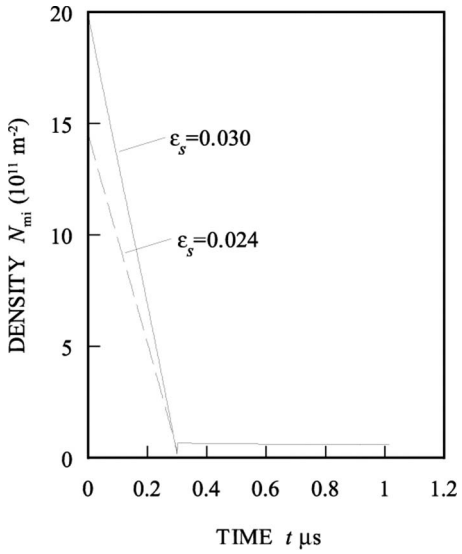

FIG. 4. Changes in time of the dislocation densities N_{mi} at the leading edge of the follower on the Asay's decay curve for ε_s=0.024 and ε_s=0.030.

$\times 10^{12}$ m^{-2} would provide the maximum value of the density that can be evaluated on the decay curve. Based on the value of 2.0×10^{12} m^{-2}, it is decided that LiF III$_b$ has no mechanism that generates dislocations as many as those reported by Gilman,[9] Shehadeh *et al.*,[10] and Bringa *et al.*[11]

B. Consideration of the anomaly

Vorthman and Duvall[3] estimated the density in the bulk of about 10^{10} m^{-2} in the postshock analysis of a LiF sample impacted at a projectile velocity of 186 m/s. The value of 10^{10} m^{-2} is not significantly larger than the preshock value $(1-5)\times 10^{9}$ m^{-2}. In short, the high densities at a projectile velocity of 340 m/s predicted by Duvall and co-workers were not observed in their recovery experiments.

The value of 10^{10} m^{-2} measured by Vorthman and Duvall[3] is considerably smaller than a maximum value of N_{mi} of 2.0×10^{11} on the Sano's decay curve and that of 2.0×10^{12} m^{-2} (1.9×10^{12} m^{-2} for D=0) on the Asay's decay curve. The main reason for this may lie in the difference between two impact velocities of 186 m/s in their experiment and 340 m/s in this analysis. In short, it is inferred from the mechanism in LiF III$_b$ by which many dislocations are not generated that the density is of the order of 10^{10} m^{-2} at the velocity of 186 m/s.

VI. CONCLUSIONS

The calculations of the dislocation density on the decay curve in LiF III$_b$ indicated that many dislocations were not generated in the material through the predicted maximum value of the density of at most 2.0×10^{12} m^{-2} at a projectile velocity of 340 m/s. On the other hand, the value of the density measured by Vorthman and Duvall was about 10^{10} m^{-2} at a projectile velocity of 186 m/s. The mechanism in the material that does not generate many dislocations suggests that the measured value is not unreasonable. It is inferred from this suggestion that the difference in values between both the densities of 2.0×10^{12} and 10^{10} m^{-2} is caused by the difference in the projectile velocity between 340 and 186 m/s and therefore that the precursor decay anomaly does not exist.

APPENDIX: DECAY CURVE FOR STRAIN

The decay curve for strain $\varepsilon_i(q)$ that was formulated by Sano[8] is described. A quadratic equation and a linear equation are connected at $q=q_1$ under the condition that the slopes of the quadratic and linear curves are equal there,

$$\varepsilon_i(q) = aq^2 + bq + c \quad (0 \leqslant q < q_1),$$

$$\varepsilon_i(q) = dq + e \quad (q \geqslant q_1),$$

where

$$a = \frac{\varepsilon_s - \varepsilon_1}{q_1^2} + \frac{d}{q_1}, \quad b = d - 2aq_1, \quad c = \varepsilon_s,$$

$$d = \frac{\varepsilon_1 - \varepsilon_2}{q_1 - q_2}, \quad e = \varepsilon_1 - dq_1,$$

where $0<q_1<q_2$, $\varepsilon_s \equiv (\varepsilon_i)_s$ is the strain at $q=0$ on the Sano's decay curve, and $\varepsilon_1 \equiv (\varepsilon_i)_1$ and $\varepsilon_2 \equiv (\varepsilon_i)_2$ are the strains at $q=q_1$ and $q=q_2$ that are also on the Asay's decay curve.

The values of ε_s, ε_1, and ε_2 that were determined by Sano[8] are described. Relation $\varepsilon_s=[u_s]\tilde{u}_{\max}/c_m$ is derived from the RH jump condition $\tilde{u}_s=c_m\varepsilon_s$, where $\tilde{u}_s \equiv (\tilde{u}_i)_s$, $[u_s]=\tilde{u}_s/\tilde{u}_{\max}$, $c_m \cong (c_f+c)/2$, and $\tilde{u}_{\max}$ is the peak particle velocity at the impact surface. First, value $[u_s]\cong 0.39$ is obtained from $[u_s]=(\tilde{u}_{RH}/\tilde{u}_{\max})[u_s]_R$ using the value $[u_s]_R \equiv u_s/\tilde{u}_{RH}=0.31$, which was determined in Ref. 7, and the value $\tilde{u}_{RH}/\tilde{u}_{\max}\cong 1.25$, which was found in Fig. 4(b) in Ref. 7. Then, value $\varepsilon_s=0.92\times 10^{-2}$ is obtained from $\varepsilon_s=[u_s]\tilde{u}_{\max}/c_m$ using the value $[u_s]\cong 0.39$ and the value $\tilde{u}_{\max}\cong 166$ m/s, which was measured using an interferometer.[18] On the other hand, on the Asay's decay curve,[1] the value of $[u_i]$ is equal to the measured value $[i_i]$ at the same time, where $[i_i]=i/i_{\max}$, where $i_{\max}$ is the peak current at the impact surface.[7] The values of $q_1=3\times 10^{-7}-t_s$ and $q_2=10^{-6}-t_s$ s are taken. Value $\varepsilon_1=0.68\times 10^{-2}$ is obtained from $\varepsilon_1=[u_i]_1\tilde{u}_{\max}/c_m$ using $[i_i]_1=[u_i]_1\cong 0.27$ in LiF, and value $\varepsilon_2=0.43\times 10^{-2}$ is obtained using $[i_i]_2=[u_i]_2\cong 0.16$.

The values of coefficients d and e are first determined using the values of ε_1 and ε_2, and those of coefficients a, b, and c are then determined.

[1] J. R. Asay, G. R. Fowles, G. E. Duvall, M. H. Miles, and R. F. Tinder, J. Appl. Phys. **43**, 2132 (1972).
[2] Y. M. Gupta, G. E. Duvall, and G. R. Fowles, J. Appl. Phys. **46**, 532 (1975).
[3] J. E. Vorthman and G. E. Duvall, J. Appl. Phys. **53**, 3607 (1982).
[4] G. Meir and R. J. Clifton, J. Appl. Phys. **59**, 124 (1986).
[5] Y. Partom, J. Appl. Phys. **59**, 2716 (1986).
[6] Y. Sano, J. Appl. Phys. **77**, 3746 (1995).
[7] Y. Sano, J. Appl. Phys. **85**, 7616 (1999).
[8] Y. Sano, J. Appl. Phys. **88**, 1818 (2000).
[9] J. J. Gilman, Mech. Mater. **17**, 83 (1994).
[10] M. A. Shehadeh, H. M. Zbib, and T. Diaz De La Rubia, Philos. Mag. **85**, 1667 (2005).
[11] E. M. Bringa, K. Rosolankova, R. E. Rudd, B. A. Remington, J. S. Wark, M. Duchaineau, D. H. Kalantar, J. Hawreliak, and J. Belak, Nature Mater. **5**, 805 (2006).

[12]Y. Sano and I. Miyamoto, J. Math. Phys. **41**, 6233 (2000).
[13]G. E. Duvall, in *Stress Waves in Anelastic Solids*, edited by H. Kolsky and W. Prager (Springer, Berline, 1964), p. 20.
[14]G. R. Fowles and R. F. Williams, J. Appl. Phys. **41**, 360 (1970).
[15]R. W. Armstrong, W. Arnold, and F. J. Zerilli, J. Appl. Phys. **105**, 023511 (2009).
[16]A. V. Granato, in *Metallurgical Effects at High Strain Rates*, edited by R. W. Rohde, B. M. Butcher, J. R. Holland, and C. H. Karnes (Plenum, New York, 1973), p. 255.
[17]O. E. Jones and J. D. Mote, J. Appl. Phys. **40**, 4920 (1969).
[18]J. R. Asay, D. L. Hicks, and D. B. Holdridge, J. Appl. Phys. **46**, 4316 (1975).